

Competition between charge order and superconductivity in

$$\text{La}_{2-x}\text{Ba}_x\text{CuO}_4 \quad (x \approx 1/8)$$

Jungho Kim,¹ A. Kagedan,¹ G. D. Gu,² C. S. Nelson,³ T. Gog,⁴ D. Casa,⁴ and Young-June Kim^{1,*}

¹*Department of Physics, University of Toronto,
Toronto, Ontario M5S 1A7, Canada*

²*Department of Condensed Matter Physics and Materials Science,
Brookhaven National Laboratory, Upton, New York, 11973-5000*

³*National Synchrotron Light Source,
Brookhaven National Laboratory, Upton, New York, 11973-5000*

⁴*CMC-CAT, Advanced Photon Source,
Argonne National Laboratory, Argonne, Illinois 60439*

(Dated: February 8, 2020)

Abstract

We have carried out a detailed investigation of the temperature and magnetic field dependence of charge ordering in $\text{La}_{2-x}\text{Ba}_x\text{CuO}_4$ ($x \approx 1/8$) utilizing high-resolution x-ray scattering. We find that the charge order correlation length exhibits unusual temperature and magnetic field dependence. Specifically, at zero field the correlation length gets smaller as the temperature is decreased below ~ 12 K, and it grows back as the magnetic field greater than ~ 5 T is applied in the superconducting phase. This observation suggests that the charge ordering is closely related to the recently discovered two-dimensional superconductivity in this material.

PACS numbers: 61.10.-i, 74.72.Dn, 71.45.Lr, 61.10.-i

Charge inhomogeneity in strongly correlated electron systems such as the cuprate superconductors has drawn much attention for its intimate relationship with exotic charge transport properties [1, 2]. In particular, neutron scattering experiments have revealed that doped holes arrange themselves in orderly rows in the copper oxide plane in certain high-temperature superconductors. This static ordering of charge stripes and associated spin stripes was first observed in $\text{La}_{1.6-x}\text{Nd}_{0.4}\text{Sr}_x\text{CuO}_4$ (LNSCO) crystals [3, 4, 5]. More recently, stripe ordering has been investigated in detail in $\text{La}_{1.875}(\text{Ba}, \text{Sr})_{0.125}\text{CuO}_4$ [6, 7, 8, 9]. In other materials, such stripes may also exist, although in most cases the stripes are not static and fluctuate with time and position [10]. Understanding the role of stripe physics in cuprate superconductors is believed to be essential in elucidating the superconducting mechanism of the cuprates.

Despite the fundamental importance of charge ordering in the cuprates, only a limited number of experiments have been carried out to study charge stripes [7, 9, 11, 12] and a comprehensive examination of the relationship between charge stripes and superconductivity is still lacking. We note that there have been extensive neutron scattering studies on spin stripe correlations, including measurements of their temperature and magnetic field dependence [13, 14, 15], while scanning tunneling spectroscopy experiments have shown intricate real space images of checker-board type charge distribution in a number of cuprate superconductors [16, 17]. However, no systematic field dependence study of charge ordering has been carried out to date.

We have carried out a detailed investigation of temperature and magnetic field dependence of charge order (CO) in $\text{La}_{2-x}\text{Ba}_x\text{CuO}_4$ ($x \approx 1/8$) (LBCO) utilizing high-resolution x-ray scattering. We find that the correlation length of the charge order exhibits unusual temperature and magnetic field dependence. Specifically, at zero field the correlation length decreases as the sample is cooled below ~ 12 K, while it increases as magnetic field greater than ~ 5 T is applied in the superconducting phase. These observations suggest that the charge ordering is closely related to the recently discovered two-dimensional superconductivity in this material [18]. This finding also shows that static charge order competes with the superconducting ground state, and emphasizes the role of quantum fluctuations in cuprates in agreement with recent experiments [19, 20].

The magnetic field dependence was studied at the X21 beamline at the National Synchrotron Light Source (NSLS). The beamline is equipped with a superconducting magnet

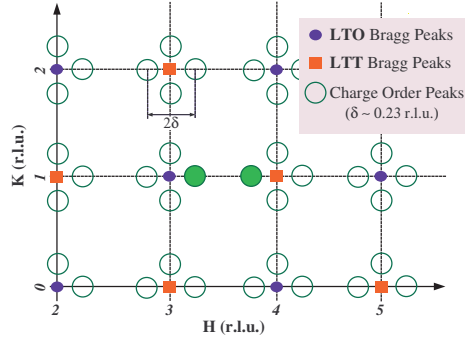


FIG. 1: (Color online) Schematic representation of the $(H,K,0)$ plane of reciprocal space. Blue filled circles and red filled squares represent LTO and LTT peak, respectively (See the text for explanation). Large open circles (green) correspond to the positions where CO peaks are located. The filled green circles indicate the CO peaks investigated in the current study.

that can provide a magnetic field of up to $\mu_0 H = 10$ T and temperatures as low as $T = 2$ K. The incoming photon with energy 15 keV was selected by a double bounce Si(111) monochromator, and horizontal scattering geometry was used. In order to reduce the background and to improve the resolution, a LiF(200) analyzer crystal was placed in the scattering geometry after the sample. While preliminary x-ray scattering experiments were carried out at the X22C beamline at NSLS, the high-resolution temperature dependence data were obtained at the 9ID at the Advanced Photon Source (APS). For the temperature dependence study at APS, a Si(111) crystal was used as both the monochromator and the analyzer, and the photon energy was 12 keV. The sample was mounted on a closed-cycle He refrigerator which could reach a base temperature of about 7.5 K. The LBCO sample used in our measurements was grown by the traveling-solvent floating zone technique at Brookhaven National Laboratory. The superconducting onset, T_c , of the particular sample studied here was measured to be approximately 6 K.

Fig. 1 shows a schematic (H,K) plane of the reciprocal space of LBCO. Filled circles represent the points where Bragg peaks are found in the low temperature orthorhombic (LTO) phase, and filled squares are the points where additional Bragg reflections occur in the low temperature tetragonal (LTT) phase below ~ 60 K. Large open circles represent the (H,K) positions of the incommensurate superlattice peaks arising from the static CO. Note that these CO peaks occur at the half-integer L values, reflecting the criss-crossing pattern of the stripes [11]. Detailed investigation of the magnetic field ($\mu_0 H$) dependence

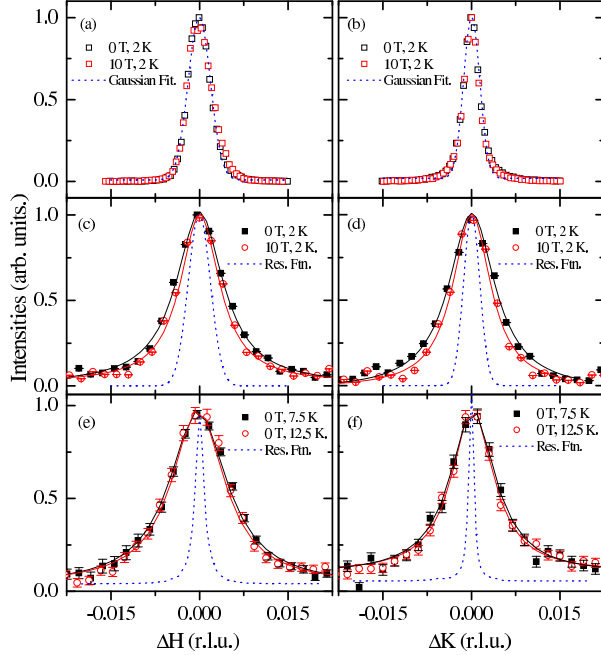


FIG. 2: (Color online) (a) and (b) show H and K scans, respectively, of the (4 1 0) Bragg peak for $\mu_0 H=0$ T and 10 T at T=2 K. The dotted lines are Gaussian fits to the raw data. (c) and (d) show H and K scans, respectively, of the (3.77, 1, 0) superlattice peak for $\mu_0 H=0$ T and 10 T at T=2 K. (e) and (f) show H and K scans, respectively, of the (3.23, 1, 5) peak for T=7.5 K and 12.5 K at zero field. The solid lines in (c)-(f) are fits to a Lorentzian function convoluted with the instrumental resolution which is shown as a dotted line.

was carried out near (3.77,1,0.5), while the temperature dependence study was focused on the (3.23,1,5.5) peak [21].

The sample was cooled in zero-field to 2 K, which is well below the superconducting and the CO temperature of ~ 6 K and ~ 50 K, respectively. The magnetic field was applied perpendicular to the CuO_2 plane, which coincides with the scattering plane within 2 degrees. The representative scans along the H and K directions of the (3.77,1,0.5) peak for two magnetic field values of $\mu_0 H=0$ T and 10 T at T=2 K are shown in Figs. 2(c) and (d), respectively. The statistical error bars are much smaller than the symbol size in the figure. To facilitate easy comparison of the width change, all scans are plotted as a function of relative momentum transfer, $(\Delta H, \Delta K)$, and are normalized to have matching peak heights.

We can see that the CO peak width is not resolution limited, unlike the Bragg peak whose width is limited by the instrumental resolution. In fact, the width of the CO peak is

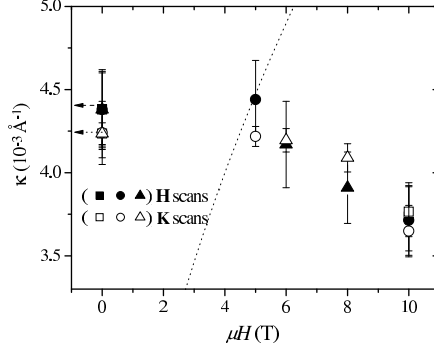


FIG. 3: The magnetic field ($\mu_0 H$) dependence of the (3.77,1,0) CO peak widths along the H and K direction. Filled and open symbols are κ_H and κ_K , respectively. Three different measurements with different combinations of magnetic fields were performed as described in the text. The dashed line is the inverse of vortex lattice parameter ($1/a_0$) as discussed in the text.

about twice that of the instrumental resolution which is shown as a dotted line in Figs. 2(c) and (d). In particular, one can clearly see the sharpening of the peak in both the H and K directions under applied magnetic field. This change is not very large (between 10 and 20 %), but based on several tests described below, we believe that this effect is not due to experimental uncertainties.

Firstly, in Figs. 2(a) and (b), we show similar H and K scans for the nearby (4, 1, 0) Bragg peak as a comparison. Both the Bragg peak and the CO peak data were obtained with the same experimental conditions in one setting. In contrast to the CO peak widths, the Bragg peak widths in both the H and K directions are found to remain unchanged with applied magnetic field up to 10 T. Secondly, the measurement was repeated three times using different combinations of magnetic fields. The first run measured the CO peak widths at fields of 0 T and 10 T as displayed in Figs. 2(c) and (d), respectively. The second run measured the peak widths at fields of 0 T, 5 T, and 10 T and the third run at fields of 0 T, 6 T, and 8 T. After each run, the sample was warmed above the CO temperature to eliminate the possibility of sample history dependence [22]. All three runs showed the same magnetic field dependence of the CO peak width. Thirdly, as described below, we have also observed changes in the CO peak width in our temperature dependence study, which is consistent with the physical picture illustrated by the field dependence.

To see how the intrinsic peak width of the (3.77,1,0.5) superlattice reflection changes with magnetic field, the scans shown in Figs. 2(c) and (d) are fitted to a two-dimensional

Lorentzian peak convoluted with the instrumental resolution which was obtained by fitting the (4,1,0) Bragg peak to a Gaussian function. The resulting half-width at half maximum (HWHM, κ) values are summarized in Fig. 3. Filled and open symbols correspond to κ_H and κ_K , respectively. One can immediately notice that the CO correlation is quite isotropic in the copper oxide plane, which is due to the fact that the stripes on neighboring layers run perpendicular to each other [4]. The values of both κ_H and κ_K at $\mu_0 H=0$ T are approximately $0.0043(3)\text{\AA}^{-1}$, corresponding to a correlation length of $\sim 230\text{\AA}$, which is consistent with results reported earlier [9]. With an increase in $\mu_0 H$, the peak width decreases, which becomes noticeable above $\mu_0 H=5$ T. At 10 T, κ_H (or κ_K) is about $0.0037(2)\text{\AA}^{-1}$, corresponding to a correlation length of $\sim 270\text{\AA}$, which is about 17% larger than the zero-field value. This change in the correlation lengths corresponds to the correlation area growing from about 3500 unit cells at 0 T to nearly 5000 unit cells at 10 T, an expansion of almost 37 %.

It is interesting to note that this “critical” field of ~ 5 T corresponds to the field at which the vortex lattice spacing becomes comparable to the CO correlation length. Using the available neutron scattering data for $\text{La}_{2-x}\text{Sr}_x\text{CuO}_4$ [23, 24, 25], one can write the vortex lattice spacing as $a_0 \sim 500/\sqrt{\mu_0 H}$ in \AA with $\mu_0 H$ in T. This empirical relationship is plotted as a dashed line in Fig. 3. One can see that the CO correlation length does not change at small field, but starts to increase when the separation between vortices become similar to the CO correlation length.

In addition to magnetic field dependence, we have carried out temperature dependence measurements of the CO peak at zero field, focusing specifically on the low temperature region. Representative H and K scans of the (3.23,1,5.5) peak are shown in Figs. 2(e) and (f), respectively, at temperatures $T=7.5$ K and 12.5 K. For these scans, the Si(111) analyzer was utilized to achieve much better instrumental resolution, which is shown as dotted lines in the figure. Not surprisingly, the resulting CO peak widths are consistent with the values obtained with a different experimental setup. However, the change of the peak width in these scans is not obviously identifiable, although fitting results suggest a small decrease of the peak widths as the temperature is lowered.

In fact, far better insight into the temperature dependence of the CO peak can be achieved by observing the temperature dependence of the peak intensity and the integrated intensity. At each temperature, the H and K scans as shown in Figs. 2(e) and (f) are fitted to a

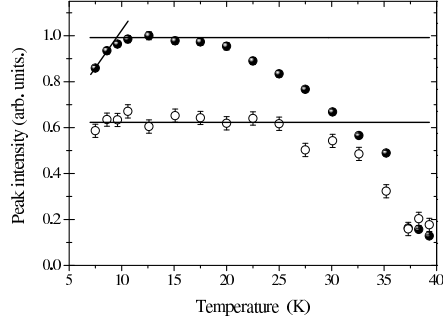


FIG. 4: The temperature dependent change of the (3.23,1,5.5) CO peak intensity. The integrated intensity of the peak, which is proportional to the stripe order parameter squared, is also included. The peak intensity exhibits a significant decrease below approximately 12 K while the integrated intensity remains unchanged.

2D Lorentzian function convoluted with the instrumental resolution function. The peak intensity is the amplitude of the Lorentzian function. In Fig. 4, we plot the peak intensity of the (3.23,1,5.5) CO peak as a function of temperature. In this plot, we also show the integrated intensity of the peak, which is proportional to the CO order parameter squared.

The integrated intensity is saturated below approximately 30 K, indicating that the lattice distortion due to the CO itself does not change much below this temperature. However, the peak intensity exhibits a significant decrease below approximately 12 K. Due to experimental constraints, we were only able to obtain data at temperatures above 7.5 K, which is just above T_c . However, preliminary measurements down to 2 K also show qualitatively similar behavior. We have also observed the same temperature dependence of other CO peaks. Since the integrated intensity remains the same at these temperatures, the peak intensity drop is entirely due to the change in the peak widths [26]. That is, as the temperature is lowered, the CO peak becomes broader in both H and K directions. Therefore, the CO correlated region seems to shrink in size as temperature is lowered below 12 K, while not much change is observed above this temperature.

This temperature dependence is slightly different from the observed field dependence at low temperatures: the correlation length remains constant in the low field phase, and grows when the field is increased above the threshold of ~ 5 T. Although this might indicate that the observed correlation length dependence on the field and temperature has different underlying physics, it is not unreasonable to assume that they have common origin. In fact, we would like to argue that the observed field and temperature dependence of the CO corre-

lation length is manifestation of a phase transition (or crossover) from the low temperature CO-suppressed phase to high temperature phase in which CO correlation is allowed to grow. A candidate for such phase transition has been discovered in a recent study of the transport properties of LBCO by Li and coworkers [18]. They observed that strong two-dimensional (2D) superconducting fluctuations exist below the stripe ordering temperature, and that 2D superconductivity sets in at lower temperatures. We note that the 2D superconducting regime in their H-T phase diagram almost coincides with the region in which the CO correlation length is minimized in our study, strongly suggesting that the observed variation of the CO correlation length could be closely related to the experimental signatures of the 2D superconductivity. Since the CO correlation length decreases in the 2D superconducting phase, it is natural to expect that the CO competes with the 2D superconductivity. The CO correlation can be enhanced apparently, as 2D superconductivity is destroyed by phase fluctuations. Experimental signatures of strong quantum fluctuations just outside superconducting phase have been observed in previous studies of Nernst effect and also magnetization [19, 20].

Alternative interpretation of our observation is also possible. In particular, one can imagine that the charge order and the superconducting order exist in spatially distinct regions of the sample, and competition between these phases drive the subtle change in their respective domain size. This picture of microscopic phase separation was first suggested by Uemura *et al.* based on their muon spin rotation (μ SR) study of the Zn substituted cuprates [27, 28]. In their recent μ SR investigation of $(\text{La, Eu, Sr})_2\text{CuO}_4$, Kojima and coworkers proposed that static stripe magnetism occurs in different spatial regions than the superconductivity [29].

Recently, Sachdev and Demler considered the effect of a thermally fluctuating superconductor on the competing order [30], and predicted that there may be a regime of temperatures near the onset of superconductivity where the charge order is enhanced with increasing temperatures. Specifically, the CO correlation area (ξ^2) is predicted to show a linear temperature dependence in the region just above T_c . The peak intensity plotted in Fig. 4 in this temperature regime is also expected to exhibit a linear temperature dependence, since the peak intensity is proportional to the correlation area (ξ^2). At present, it is difficult to conclude that the temperature dependence at low temperature ($T < 10$ K) is linear, although LBCO qualitatively exhibits the behavior expected of a system with competing superconducting and charge order.

In summary, we have observed that the correlation length of the charge order in the superconducting phase of $\text{La}_{2-x}\text{Ba}_x\text{CuO}_4$ ($x \approx 1/8$) increases with increasing magnetic field and temperature, which suggests that static charge order is suppressed in this regime. We find that this low temperature, low field region of phase diagram, where charge order is inhibited coincides with the recently discovered two-dimensional superconducting phase in this material.

We would like to thank S. Kivelson, S. Sachdev, and J. Tranquada for invaluable discussions, S. LaMarra for the work at NSLS. Research at the University of Toronto was supported by the Natural Sciences and Engineering Research Council of Canada. Work at Brookhaven was supported by the U. S. DOE, Office of Science Contract No. DE-AC02-98CH10886. Use of the Advanced Photon Source was supported by the U. S. DOE, Office of Science, Office of Basic Energy Sciences, under Contract No. W-31-109-ENG-38.

* Electronic address: yjkim@physics.utoronto.ca

- [1] J. Orenstein and A. J. Millis, *Science* **288**, 468 (2000).
- [2] E. Dagotto, *Science* **309**, 257 (2005).
- [3] J. M. Tranquada, B. J. Sternlib, J. D. Axe, Y. Nakamura, and S. Uchida, *Nature* **375**, 561 (1995).
- [4] J. M. Tranquada, J. D. Axe, N. Ichikawa, Y. Nakamura, S. Uchida, and B. Nachumi, *Phys. Rev. B* **54**, 7489 (1996).
- [5] J. M. Tranquada, N. Ichikawa, and S. Uchida, *Phys. Rev. B* **59**, 14712 (1999).
- [6] M. Fujita, H. Goka, K. Yamada, and M. Matsuda, *Phys. Rev. B* **66**, 184503 (2002).
- [7] H. Kimura, H. Goka, M. Fujita, Y. Noda, K. Yamada, and N. Ikeda, *Phys. Rev. B* **67**, 140503(R) (2003).
- [8] M. Fujita, H. Goka, K. Yamada, J. M. Tranquada, and L. P. Regnault, *Phys. Rev. B* **70**, 104517 (2004).
- [9] P. Abbamonte, A. Rusydi, S. Smadici, G. D. Gu, G. A. Sawatzky, and D. L. Feng, *Nature Phys.* **1**, 155 (2005).
- [10] E. S. Božin, G. H. Kwei, H. Takagi, and S. J. L. Billinge, *Science* **84**, 5856 (2000).
- [11] M. v. Zimmermann, A. Vigliante, T. Niemoller, N. Ichikawa, T. Frello, J. Madsen, P. Wochner,

- S. Uchida, N. H. Andersen, J. M. Tranquada, et al., *Europhys. Lett.* **41**, 629 (1998).
- [12] T. Niemöller, N. Ichikawa, T. Frello, H. Hunnefeld, N. Andersen, S. Uchida, J. Schneider, and J. Tranquada, *Europhys. Lett.* **12**, 509 (1999).
- [13] S. Katano, M. Sato, K. Yamada, T. Suzuki, and T. Fukase, *Phy. Rev. B* **62**, R14677 (2000).
- [14] B. Lake, G. Aeppli, K. N. Clausen, D. F. McMorrow, K. Lefmann, N. E. Hussey, N. Mangkorntong, M. Nohara, H. Takagi, T. E. Mason, et al., *Science* **291**, 1759 (2001).
- [15] B. Khaykovich, R. J. Birgeneau, F. C. Chou, R. W. Erwin, M. A. Kastner, S.-H. Lee, Y. S. Lee, P. Smeibidl, P. Vorderwisch, and S. Wakimoto, *Phys. Rev. B* **67**, 054501 (2003).
- [16] J. E. Hoffman, K. McElroy, D.-H. Lee, K. M. Lang, H. Eisaki, S. Uchida, and J. C. Davis, *Science* **295**, 466 (2002).
- [17] T. Hanaguri, C. Lupien, Y. Kohsaka, D.-H. Lee, M. Azuma, M. Takano, H. Takagi, and J. C. Davis, *Nature* **430**, 1001 (2004).
- [18] Q. Li, M. Hucker, G. D. Gu, A. M. Tsvelik, and J. M. Tranquada, *Phys. Rev. Lett.* **99**, 067001 (2007).
- [19] Y. Wang, L. Li, and N. P. Ong, *Phys. Rev. B* **73**, 024510 (2006).
- [20] L. Li, J. G. Checkelsky, S. Komiya, Y. Ando, and N. P. Ong, *Nature Phys.* **3**, 311 (2007).
- [21] We were able to observe CO peaks at most of these (H,K) positions shown in green circles.
- [22] In this study, we have not systematically investigated the history dependence.
- [23] B. Keimer, W. Y. Shih, R. W. Erwin, J. W. Lynn, F. Dogan, and I. A. Aksay, *Phys. Rev. Lett.* **73**, 3459 (1994).
- [24] B. Lake, H. M. Ronnow, N. B. Christensen, G. Aeppli, K. Lefmann, D. F. McMorrow, P. Vorderwisch, P. Smeibidl, N. Mangkorntong, T. Sasagawa, et al., *Nature* **415**, 299 (2002).
- [25] R. Gilardi, J. Mesot, A. Drew, U. Divakar, S. L. Lee, E. M. Forgan, O. Zaharko, K. Conder, V. K. Aswal, C. D. Dewhurst, et al., *Phys. Rev. Lett.* **88**, 217003 (2002).
- [26] The peak intensity drop ($\sim 12\%$) is consistent with the small decrease ($\sim 10\%$) observed in the width of Fig. 2(e) and (f).
- [27] B. Nachumi, A. Keren, K. Kojima, M. Larkin, G. M. Luke, J. Merrin, O. Tchernyshov, Y. J. Uemura, N. Ichikawa, M. Goto, et al., *Phys. Rev. Lett.* **77**, 5421 (1996).
- [28] Y. J. Uemura, *J. Phys.: Condes. Matter* **16**, S4515 (2004).
- [29] K. M. Kojima, S. Uchida, Y. Fudamoto, I. M. Gat, M. I. Larkin, Y. J. Uemura, and G. M. Luke, *Physica B* **326**, 316 (2003).

[30] S. Sachdev and E. Demler, Phys. Rev. B **69**, 144504 (2004).